

Convergence in leaf size versus twig leaf area scaling: do plants optimize leaf area partitioning?

Duncan D. Smith^{1,†,*}, John S. Sperry¹ and Frederick R. Adler¹

¹Department of Biology, University of Utah, Salt Lake City, UT 84112, USA

[†]Present address: Department of Botany, University of Wisconsin - Madison, Madison, WI 53706, USA

*For correspondence. E-mail ddsmith3@wisc.edu

Received: 5 July 2016 Returned for revision: 15 September 2016 Accepted: 26 September 2016 Published electronically: 27 December 2016

- **Background and Aims** Corner's rule states that thicker twigs bear larger leaves. The exact nature of this relationship and why it should occur has been the subject of numerous studies. It is obvious that thicker twigs should support greater total leaf area (A_{twig}) for hydraulic and mechanical reasons. But it is not obvious why mean leaf size (\bar{A}) should scale positively with A_{twig} . We asked what this scaling relationship is within species and how variable it is across species. We then developed a model to explain why these relationships exist.
- **Methods** To minimize potential sources of variability, we compared twig properties from six co-occurring and functionally similar species: *Acer grandidentatum*, *Amelanchier alnifolia*, *Betula occidentalis*, *Cornus sericea*, *Populus fremontii* and *Symphoricarpos oreophilus*. We modelled the economics of leaf display, weighing the benefit from light absorption against the cost of leaf tissue, to predict the optimal $\bar{A} : A_{\text{twig}}$ combinations under different canopy openings.
- **Key Results** We observed a common \bar{A} by A_{twig} exponent of 0.6, meaning that \bar{A} and leaf number on twigs increased in a specific coordination. Common scaling exponents were not supported for relationships between any other measured twig properties. The model consistently predicted positive \bar{A} by A_{twig} scaling when twigs optimally filled canopy openings. The observed 0.6 exponent was predicted when self-shading decreased with larger canopy opening.
- **Conclusions** Our results suggest Corner's rule may be better understood when recast as positive \bar{A} by A_{twig} scaling. Our model provides a tentative explanation of observed \bar{A} by A_{twig} scaling and suggests different scaling may exist in different environments.

Key words: Allometry, Corner's rule, economics, intraspecific, leaf size, light interception, optimization, self-shading.

INTRODUCTION

In 1949, Corner identified two basic properties of plant architecture: (1) larger leaves are borne on thicker stems and (2) plants with thicker stems are less densely branched. His claim led to numerous tests of 'Corner's rules' within and across species and environments, and to explanations for why such rules would have evolved (e.g. White, 1983a, b; Brouat *et al.*, 1998; Westoby and Wright, 2003; Olson *et al.*, 2009; Yang *et al.*, 2014). The second rule may be easily explained as a corollary of area-preserving branching (McMahon and Kronauer, 1976; Sone *et al.*, 2009; Eloy, 2011). Cross-sectional stem area is approximately preserved across branch junctions, so a given trunk area will support a similar total cross-sectional area of twigs. This means that a trunk could support many narrow twigs or a few thick ones. Fewer twigs require fewer branching junctions, and hence Corner's second rule that thicker twigs show less dense branching.

At first glance, Corner's first rule seems equally simple to explain: larger leaves require thicker twigs to support their greater transportational and mechanical needs (White, 1983b; Farnsworth and Van Gardingen, 1995; Preston and Ackerly, 2003; Wright *et al.*, 2006). The complication is that twigs bear multiple leaves. So while it follows that twig dimensions should scale with total twig leaf area (A_{twig}), it is not obvious why twig

dimensions should scale with individual leaf size (\bar{A} = mean leaf size, cm^2). Thicker twigs will have greater A_{twig} , but this could be achieved regardless of whether \bar{A} increases, decreases or stays the same. Corner's first rule is peculiar in requiring that \bar{A} increases with A_{twig} . Therefore, we ask two questions: (1) how variable is the positive scaling between individual leaf size and twig leaf area; and (2) can we explain why such scaling evolved? The 'twig' in this context is defined as the current year's extension growth.

Surprisingly, in our review of the Corner's rule literature, the \bar{A} versus A_{twig} relationship is almost always overlooked (for exceptions see Falster and Westoby, 2003; Westoby and Wright, 2003). Most studies assess relationships between \bar{A} or A_{twig} and twig size, but the positive \bar{A} by A_{twig} relationship is arguably the fundamental reason why thicker twigs have larger leaves. Corner's first rule requires that \bar{A} increases with A_{twig} but it does not specify how. Suppose that \bar{A} versus A_{twig} can be described as a power function:

$$\bar{A} = a_1 A_{\text{twig}}^{b_1} \quad (1)$$

where a_1 is a scaling multiplier and b_1 is a scaling exponent. Corner's rule only requires that $b_1 > 0$. Such positive scaling could be achieved in three general ways. If the number of

leaves, $n (= A_{\text{twig}}/\bar{A})$, is constant, any changes in A_{twig} will be due to \bar{A} . Therefore, \bar{A} versus A_{twig} will be isometric ($b_1 = 1$ and $a_1 = 1/n$ in eqn (1)). Alternatively, n could decrease with greater A_{twig} , which requires \bar{A} to increase faster than A_{twig} so $b_1 > 1$. Finally, n could increase with \bar{A} and A_{twig} , making $0 < b_1 < 1$.

We assessed intraspecific \bar{A} versus A_{twig} scaling in six species to determine whether species consistently followed one of these three scaling alternatives and whether the scaling was consistent across species. These results were compared with other scaling relationships involving twig diameter (d_{twig}) and length (l_{twig}), including Corner's first rule as usually stated: \bar{A} versus d_{twig} . Although nearly all analyses of Corner's rules have used interspecific data (but see Brouat *et al.*, 1998; Preston and Ackerly, 2003), we specifically chose to determine the scaling exponent b_1 intraspecifically. The intraspecific b_1 exponent is not confounded by species-specific shifts in the a_1 multiplier (Heusner, 1982). The multiplier shifts because species can have inherently different \bar{A} from others for the same A_{twig} because of differences in habitat, natural history, phylogenetic affiliation, etc. (e.g. Givnish, 1987; Cunningham *et al.*, 1999). Our question is not why some species have different leaf sizes from others, but how and why leaf size varies with increasing twig leaf area within species. Recognizing that intraspecific b_1 could be sensitive to environment and plant functional type, we chose species that were co-occurring and functionally similar (deciduous angiosperm trees and shrubs with simple leaves and diffuse porous xylem) to test how constant b_1 was across species in ecologically and environmentally similar contexts.

The question of *how* \bar{A} scales with A_{twig} is simple to evaluate, whereas the question of *why* \bar{A} should increase with A_{twig} – much less why they may scale in a particular way – is more difficult to answer. We approached the 'why' question from an economics standpoint with the hypothesis that twigs should exhibit the optimal \bar{A} and n (and thereby A_{twig}) that maximize the net gain from the twig's complement of leaves. The net gain is the benefit from the leaves minus their cost. The benefit stems from the light energy absorbed by the leaves while the cost is based on the energy required to construct and maintain leaves. We developed a model that computed optimal \bar{A} and n for twigs with different degrees of self-shading and deployed in canopy openings of different sizes. The model was used to predict how a twig's light environment influenced the optimal \bar{A} by A_{twig} scaling. Our study follows previous efforts to model optimal leaf display (e.g. Honda and Fisher, 1978; Pearcy *et al.*, 2005), but ours is the first, to our knowledge, to use leaf display modelling to address Corner's rule.

MATERIALS AND METHODS

Location and species

All material was collected in Red Butte Canyon Natural Research Area (40.78° N, 111.81° W; 1640–1910 m.a.s.l.) located adjacent to the University of Utah in Salt Lake City. Data were collected for all species between July and September (after extension growth was complete) in 2011 and 2013. Six species were chosen from six separate eudicot orders (Judd *et al.*, 2008), including three shrubs (*Amelanchier alnifolia*,

Cornus sericea and *Symphoricarpos oreophilus*) and three trees (*Acer grandidentatum*, *Betula occidentalis* and *Populus fremontii*). Hereafter, each will be referred to by its genus name. These species were chosen due to their similarities. All are deciduous angiosperms with simple leaves and all grow within the riparian corridor. With the exception of *Symphoricarpos*, all have functionally diffuse porous xylem (Smith and Sperry, 2014).

Twig architecture

Twigs, defined as current year extension growth, were collected from larger branches cut from various individuals from each species. Trees sampled were generally <15 m tall with shallow canopies and sampled twigs were at or near the canopy periphery. Material was transported in plastic bags to the laboratory and measured the same day. Twigs with obvious damage were excluded, as were branched (syllaptic) twigs. For each twig ($n = 53\text{--}93$ per species), we recorded twig leaf area (A_{twig}), number of leaves (n), twig stem length (l_{twig}) and twig basal diameter (d_{twig} , measured at the bud scale scars at the base of the twig). Leaf areas were measured with a Li-3100 (Li-Cor, Lincoln, NE). From A_{twig} and n we calculated mean leaf size, \bar{A} . The dataset of the accessions used in the study is available as [Supplementary Data](#). Scaling relationships between all twig properties were determined using SMA (standardized major axis) line-fitting on log-transformed data via the *smatr* package (Warton *et al.*, 2012) in R 3.1.2 (R Core Team, 2014). The *smatr* package was additionally used to test for common exponents, test for isometry and perform pairwise comparisons between exponents. For pairwise comparisons, P -values were adjusted to minimize type I errors.

Economics model

The model assumes that a twig has a particular \bar{A} and n (and hence A_{twig}) because this combination maximizes net gain (benefit–cost), where benefit is a function of twig light absorption and cost is a function of twig leaf area. We assume for our purposes that the light environment experienced by a twig can be distilled to the intensity and distribution of incoming light and the level of self-shading within the twig. These properties can be represented in two dimensions. The model was written in R.

Light environment and interception

Briefly, the model approach was to make canopies of random leaves and calculate light transmission through them. We then determined the spatial autocorrelation of light transmission of each canopy and used this information to create generalized maps of canopy light transmission. We assumed twigs grow centred at the brightest point on each map. For each canopy, we calculated light absorbed by each leaf on the twig based on leaf size, light transmitted through the canopy and self-shading within the twig. More in-depth details follow.

We created two-dimensional canopies of randomly placed circular leaves at 20 mean leaf area indices ($\overline{\text{LAI}}_{\text{can}}$) between 0.5 and 5 (Fig. 1A, B). Within each random assemblage, there

were areas of little or no coverage by leaves ('canopy openings') and areas with high coverage. Twigs were assumed to grow into the canopy openings, representing a 'sun-leaf' light environment expected for the study species and their sampled twigs. To determine the spatial distribution of light penetration centred around the canopy openings (without twigs present), we discretized the simulation space into pixels and quantified canopy coverage as the number of overlapping leaves (i.e. LAI) at each pixel ($LAI_{can,pxl}$). For each pixel, the fraction of light transmitted through the canopy, $\tau_{can,pxl}$, was calculated as

$$\tau_{can,pxl} = (1 - f_{can})^{LAI_{can,pxl}} \quad (2)$$

where f_{can} is the fraction of incident light absorbed by each leaf in the canopy. We used $f_{can} = 0.5$, which is typical of individual leaves (Campbell and Norman, 1998). The $\tau_{can,pxl}$ should be spatially autocorrelated, meaning pixels with high $\tau_{can,pxl}$ should be near other pixels with high $\tau_{can,pxl}$. To generalize the spatial autocorrelation and represent it statistically, for each canopy we chose, at random, 1000 pixels (0.8 % of total) with the highest transmission (that is, pixels within canopy openings). For each random pixel, we recorded $\tau_{can,pxl}$ at 20 discrete distances away and in random directions (arrows in Fig. 1A, B).

The mean transmission versus distance, x , values were fitted with the function:

$$\bar{\tau}_{can,pxl} = a_2 \exp(b_2 x) + \bar{\tau}_{can,min} \quad (3)$$

which was used to predict the light available in and around the canopy openings where the twig would be centred (Fig. 1E, F). In eqn (3), $\bar{\tau}_{can,min}$ is the lower asymptote, which corresponds closely to the light penetration under a homogeneous canopy with \bar{LAI}_{can} . The greater $\bar{\tau}_{can,min}$, the less dense the canopy and the larger its canopy openings. For readability, $\bar{\tau}_{can,min}$ is referred to as 'canopy openness' in subsequent text and figures.

Twigs populating canopy openings were modelled as vertically oriented, unbranched stems (Fig. 1C, D). Leaves were uniform ellipses (aspect ratio = 3) arranged alternately with spiral phyllotaxy. The angle between leaves was centred on the golden angle (137.5°) with normally distributed random variation (s.d. = 5.6°). We modelled leaf sizes and numbers based on observed ranges for the study species: $\bar{A} = 0.6\text{--}83.9 \text{ cm}^2$ and $n = 1\text{--}55$. The A range was discretized into 55 logarithmically spaced values.

Light absorption by each leaf in each twig was calculated from $\bar{\tau}_{can,pxl}$ and leaf overlap within the twig. Leaf overlap was determined by discretizing the space into pixels and counting the

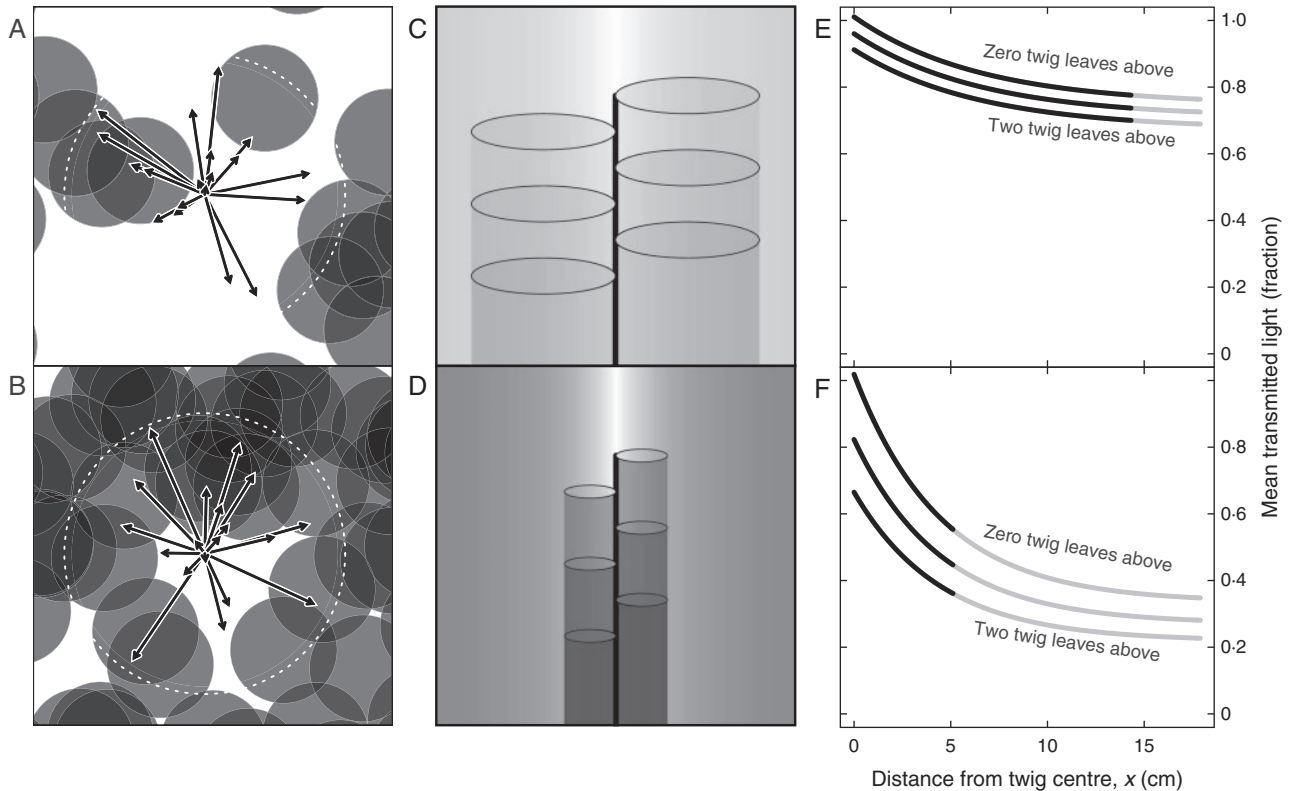


FIG. 1. Key components of the light interception model illustrated by an open canopy with low self-shading (top row) and a denser canopy with higher self-shading. The incoming light environment was modelled as randomly placed leaves at different densities (A, B). Canopy openings were quantified from incoming light in random directions at distances from points with high light (arrows) up to the maximum leaf length (dotted white circles). Under these canopies, mean incoming light decreased exponentially with distance from highest light [see horizontal gradients in (C, D) and 'zero leaves' curves in (E, F)]. Twig self-shading reduced available light to leaves lower on the twig and the amount of reduction was a function of canopy openness [see vertical gradients in (C, D) and 'leaves above' curves in (E, F)]. Curves in (E, F) indicate available light to three uppermost leaves; black portions correspond to optimal leaf size. For illustration, curves reflect perfect leaf overlap.

twig leaves above each pixel of each leaf, i ($LAI_{\text{leaf},i,\text{pxl}}$). The fraction of total light incident on each pixel of each leaf was

$$\tau_{\text{leaf},i,\text{pxl}} = \bar{\tau}_{\text{can},\text{pxl}}(1 - f_{\text{eff}})^{LAI_{\text{leaf},i,\text{pxl}}} \quad (4)$$

where f_{eff} is the effective fraction of attenuation by each leaf within the twig (see below). The absorption, α , by each pixel in each leaf is

$$\alpha_{\text{leaf},i,\text{pxl}} = \tau_{\text{leaf},i,\text{pxl}} f_{\text{leaf}} l_{\text{pxl}}^2 \quad (5)$$

where f_{leaf} ($= 0.5$) is the fraction of $\tau_{\text{leaf},i,\text{pxl}}$ absorbed and l_{pxl} is the side length of each pixel. The l_{pxl} was 0.1 mm in the smallest leaves and increased with leaf size, which meant each leaf was composed of > 5600 pixels and all leaf sizes were represented with the same level of precision. Total absorption by each leaf, i ($\alpha_{\text{leaf},i}$) and the whole twig (α_{twig}) were obtained by summing $\alpha_{\text{leaf},i,\text{pxl}}$ within leaves and then across leaves, respectively.

The effective attenuation of light within the twig, f_{eff} , was allowed to vary (Fig. 1C–F). If all light was collimated and incident parallel to the twig axis, then self-shading would be maximized and the fraction of effective attenuation should equal the fraction of absorption ($f_{\text{eff}} = f_{\text{leaf}} = 0.5$). But in reality self-shading will rarely be maximized because there is also diffuse light, leaves move, and the direction of collimated light moves relative to the twig. To simulate different degrees of self-shading, effective attenuation by leaves in the twig (f_{eff}) was decoupled from absorption by the leaves (f_{leaf}). For example, in a sparse canopy with large openings, leaves that are low on a twig may still have high integrated light absorption (i.e. μmol photosynthetically active radiation $\text{m}^{-2} \text{day}^{-1}$) even if each leaf above absorbs a large fraction of its incident light (e.g. Fig. 1, upper panels). Such a twig would have minimal self-shading. Under a denser canopy with smaller openings, the light available to the same low-positioned leaf would be much more reduced by absorption of the leaves crowding around it (greater self-shading; e.g. Fig. 1, lower panels). Based on this logic, f_{eff} (which defines the degree of self-shading) was a function of canopy openness ($\bar{\tau}_{\text{can},\text{min}}$). We defined $f_{\text{eff},\text{open}}$ for the least dense canopy with the largest openings (greatest $\bar{\tau}_{\text{can},\text{min}}$) and $f_{\text{eff},\text{closed}}$ for the densest canopy with the smallest openings (lowest $\bar{\tau}_{\text{can},\text{min}}$). The $f_{\text{eff},\text{open}}$ was assigned one of seven values from lowest to highest self-shading (0.01, 0.05, 0.1, 0.2, 0.3, 0.4, 0.5). The $f_{\text{eff},\text{closed}}$ either equalled $f_{\text{eff},\text{open}}$ (equal twig self-shading in all canopies; Fig. 5A) or was set to 0.5 (maximal self-shading in the densest canopy; Fig. 5C,E). When $f_{\text{eff},\text{closed}} = 0.5$, the f_{eff} decreased either linearly or curvilinearly with increasing openness to $f_{\text{eff},\text{open}}$ (Fig. 5C, E). For readability, we refer to f_{eff} as ‘self-shading’ in subsequent text and figures.

Predicting optimal twig properties

We defined net gain as

$$\text{net} = \text{benefit} - \text{cost} = c_0 \alpha_{\text{twig}} - c_1 n \bar{A}^\beta \quad (6)$$

The multipliers c_0 and c_1 implicitly translate light absorption and leaf area into the same metabolic currency and the

exponent β dictates how cost/area varies with \bar{A} . By default, cost/area was constant ($\beta = 1$) but we also considered increasing cost/area [$\beta > 1$; due to increasing LMA (Milla and Reich, 2007) and/or proportionally greater structural investment in larger leaves (Niinemets *et al.*, 2007; but see Villar and Merino, 2001)]. Specifically, we tested $\beta = 1.1$, the average intraspecific LMA versus leaf size exponent across 157 species (Milla and Reich, 2007). The cost of stems is intentionally ignored. In the context of woody, deciduous plants, it may be argued that building stems is a long-term investment relative to leaves and so the two do not play into the same economics equation.

As c_0 and c_1 change, net gains are altered, which can affect which $\bar{A} : n$ pair is optimal. The relative benefit of any pair depends on the c_0/c_1 ratio. Therefore, $c_1 = 1$ was generally maintained (but see next paragraph) while varying c_0 . The range for the benefit coefficient, c_0 , was selected by two criteria: (1) the c_0 must produce a positive maximum net gain within the modelled ranges of \bar{A} and n ; (2) the c_0 must meet this criterion across at least 15 of the 20 modelled canopies. Each modelled canopy typically produced a unique $\bar{A} : n : A_{\text{twig}}$ optimum, so this second criterion ensured a robust sample of \bar{A} and A_{twig} optima from which to determine the b_1 scaling exponent. For each self-shading scenario (i.e. each curve in the left panels of Fig. 5), we ran the model with 500 c_0 values over the range predicted to satisfy the first criterion. The c_0 values were binned into 100 size classes and each c_0 was then filtered on the two criteria. Bins with fewer than four $\bar{A} : n$ pairs were excluded. From the remaining simulated data, SMA regression was used to evaluate \bar{A} versus A_{twig} scaling in each c_0 bin.

Model variants

In the model presented thus far, numerous assumptions were made about twig structure and economic parameters. In order to test the generality of the model predictions, we considered several alternative assumptions. (1) Leaf phyllotaxy was made opposite with pairs separated by 90° (i.e. decussate). As with alternate, spiral phyllotaxy, random variation was added to leaf angles. Three of the six study species (*Acer*, *Cornus* and *Symphoricarpos*) had opposite leaves and the decussate pattern has been shown to reduce light absorption (Valladares and Brites, 2004). (2) Leaf sizes were varied within twigs. Sizes were chosen randomly from a normal distribution around \bar{A} (s.d. = $0.2\bar{A}$). (3) Circular leaves (aspect ratio = 1) were used in place of ellipses with aspect ratio = 3. (4) We also considered cost (via c_1) as a function of leaf light environment. Leaf mass/area and respiration/area (Posada *et al.*, 2009) and nitrogen/area (Niinemets *et al.*, 2015) have been shown to increase asymptotically with light regime. This dependency was represented with a Michaelis–Menten-like function

$$c_1 = \frac{a_3 \alpha_{\text{leaf},i} / \bar{A}}{b_3 + \alpha_{\text{leaf},i} / \bar{A}} + 1 \quad (7)$$

where the minimum is 1, the maximum is $a_3 + 1$ and b_3 is the $\alpha_{\text{leaf},i} / \bar{A}$ at which c_1 is half-way between the minimum and maximum. We varied a_3 and used $b_3 = 0.25$ because the maximum absorption per area was 0.5 ($= f_{\text{leaf}}$). Greater leaf thickness and N content should also increase leaf absorption, but

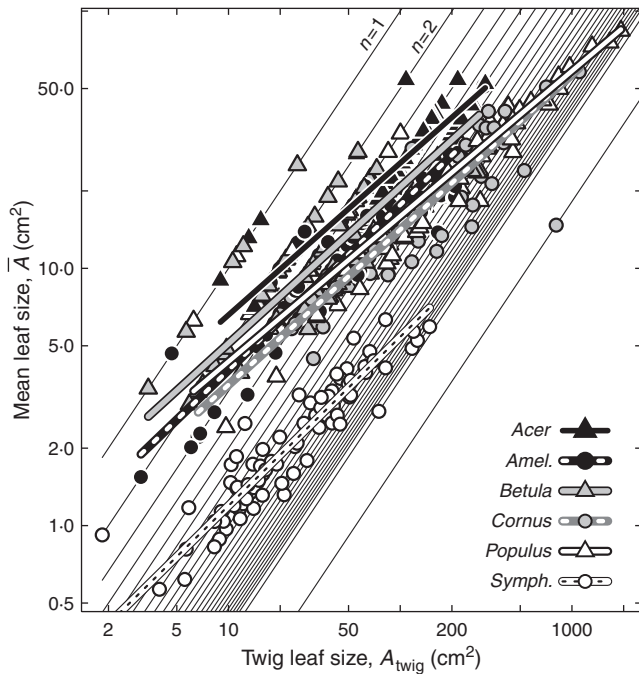


Fig. 2. Mean leaf size versus twig leaf area (\bar{A} versus A_{twig}) relationships. SMA scaling exponents were very similar across species and all less than isometric. Scaling coefficients are given in Table 1. Thin background lines are n -isoclines for observed n , which correspond to \bar{A} versus A_{twig} isometry. Triangles represent trees and circles represent shrubs.

Evans and Poorter (2001) showed that the change in absorption is small. When c_1 varied, c_0 was chosen and regressions were performed as above.

RESULTS

Twig architecture

The \bar{A} and A_{twig} were positively related within all six species (Fig. 2), as expected from Corner's first rule. SMA scaling exponents (b_1) were very similar, ranging from 0.56 to 0.66 (Table 1) with evidence of a common exponent of 0.61 ($P=0.14$). All exponents were significantly less than 1 ($P<0.001$), meaning that n increased systematically with increasing \bar{A} and A_{twig} (Fig. 2, regression lines cross thin iso- n lines). Interspecific \bar{A} by A_{twig} scaling ($b_1=0.85$) was steeper than any intraspecific value due to variation in a_1 multipliers across species (Fig. 2). The \bar{A} and A_{twig} versus n scaling exponents were more variable than \bar{A} versus A_{twig} (common exponent test, $P=0.023$ and $1.9e-3$, respectively). This lack of support for a common exponent was attributable to *Betula*, which was significantly shallower than *Symphoricarpos* in both cases and *Amelanchier* in A_{twig} versus n (Table 1). No other relationship between twig properties showed the similarity observed for \bar{A} by A_{twig} (Fig. 3; Table 1). The more traditional assessment of Corner's first rule (\bar{A} versus d_{twig}) showed variable exponents (1.24–2.41) that were far from supporting a common exponent ($P=1.0e-8$; six pairwise differences of 15 possible). The A_{twig} by d_{twig} data also showed a wide range in exponents (1.89–3.97) with no common exponent

($P=1.1e-16$; eight pairwise differences). \bar{A} and A_{twig} scaled with length (Fig. 3C, D), similarly to how they scaled with d_{twig} due to the positive scaling between l_{twig} and d_{twig} . The \bar{A} versus l_{twig} exponents were fairly narrowly distributed (range 0.35–0.61) but with four significant pairwise differences: those for *Cornus*, *Populus* and *Symphoricarpos* were steeper than those for *Betula*, while that for *Populus* was also steeper than that for *Amelanchier*.

Economics model

Across all scenarios of canopy structure and twig self-shading, \bar{A} versus A_{twig} exponents were positive, ranging from 0.52 to 1.31 overall. In other words, maximizing return on twig leaf investment predicted the Corner's rule corollary that greater A_{twig} is achieved through greater \bar{A} . Before detailing the variation in exponents, it is necessary to describe the general behaviour of the model. Results refer to twigs with homogeneous leaves unless otherwise noted. Figure 4A illustrates that, for a given light environment (i.e. canopy openness and twig self-shading) and constant n , the benefit (dashed line) and cost (grey line) increased with increasing \bar{A} . However, the benefit increased at a declining rate due to the loss of incident light as the larger leaf sizes extend beyond the canopy openings. The cost increased isometrically with \bar{A} (Fig. 4A, grey line) or steeper when exponent $\beta > 1$ (not shown). The result was that cost surpassed benefit at some \bar{A} . Before this point, net gain (Fig. 4a, black line) was positive and there was some \bar{A} that maximized net gain for this particular n and light environment. As n increased, the locally optimal \bar{A} stayed the same or decreased (Fig. 4B) and maximum net gain increased to a peak and then declined. The $\bar{A} : n : A_{\text{twig}}$ trio that maximized net gain was the optimal combination for this light environment.

The model predicted that, as canopies became less dense with larger openings (higher $\bar{\tau}_{\text{can,min}}$), the optimal \bar{A} and A_{twig} increased (Fig. 4C; see also Fig. 1C). The scaling exponent was determined from SMA regressions across these \bar{A} and A_{twig} optima. All \bar{A} by A_{twig} regressions had $r^2 > 0.86$ (mean = 0.98). The c_0 values that met our criterion of producing optimal $\bar{A} : n : A_{\text{twig}}$ under at least 15 of 20 canopies were narrowly distributed from 2.6 to 10.1 (tested range: 2.1–48.0) when $c_1 = 1$. The c_0 had a relatively minor effect on the \bar{A} by A_{twig} exponent, causing an average variation of 0.14 across the 32 different scenarios in Fig. 5.

The \bar{A} by A_{twig} exponent depended on the self-shading within the twig. When twig self-shading was constant across all canopy structures, exponents were near 1, indicating a relatively constant n . This was true regardless of the degree of self-shading (f_{eff} values; Fig. 5A, B). Increasing the leaf cost exponent, β , from 1 to 1.1 (larger leaves are more expensive) slightly steepened the \bar{A} by A_{twig} scaling (Fig. 5B, open circles).

When self-shading decreased with more open canopies (e.g. as illustrated in Fig. 5C, E), the \bar{A} by A_{twig} exponent fell below 1 (Fig. 5C–F). The steeper the decrease, the lower the exponent, especially when self-shading decreased curvilinearly (versus linearly). Decreasing self-shading was necessary for exponents to fall to the observed common value of 0.61 and below (grey bar in Fig. 5D, F). Increasing the cost of larger leaves (changing β from 1 to 1.1) tended to decrease the exponent but only

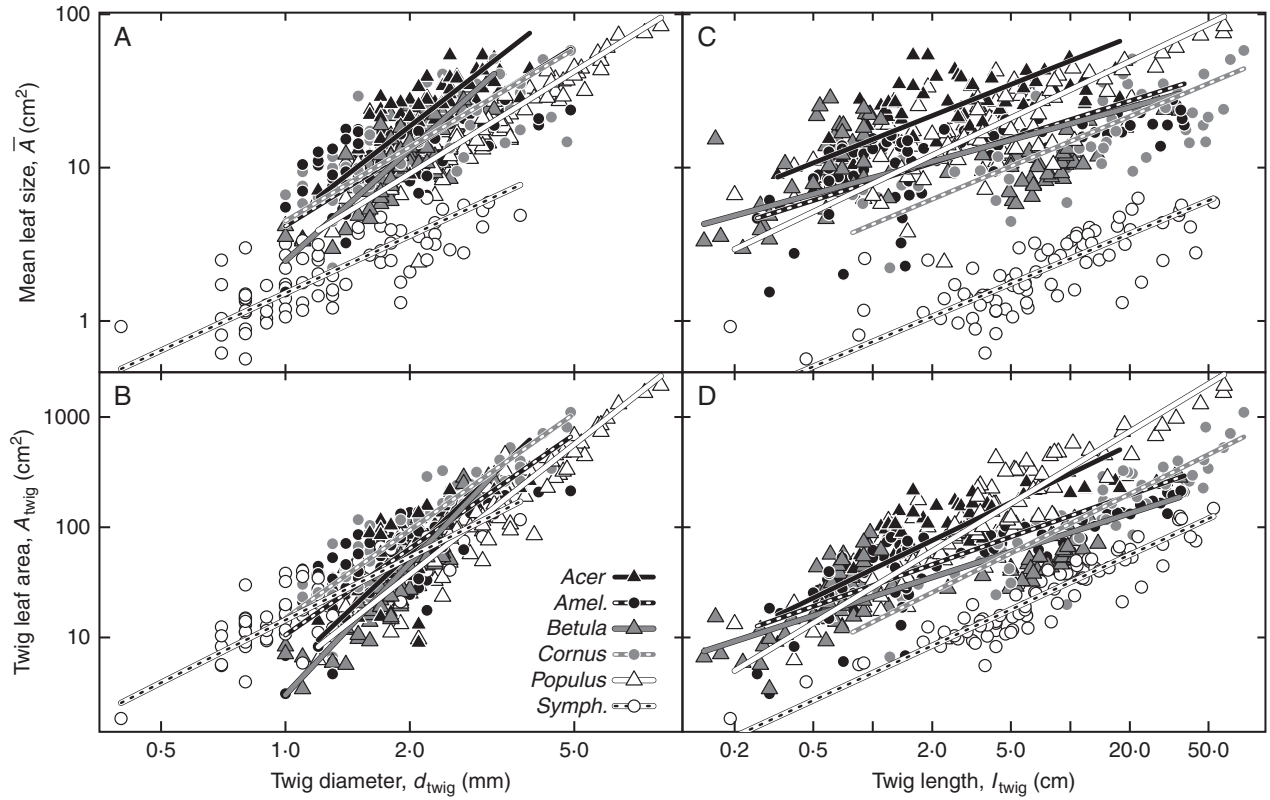


FIG. 3. Mean leaf size and twig leaf area were well correlated with twig diameter and length within species. However, the SMA regressions (shown) had very different exponents. Scaling coefficients and common exponent tests are shown in Table 1. Triangles indicate tree species and circles represent shrubs.

TABLE 1. SMA regressions between all measured twig structure parameters in each species and results from common exponent tests (table sorted by test P-value). Pairwise differences were evaluated using $P = 0.05$ as a threshold for adjusted P-values. Units: areas in cm^2 ; diameters in mm; lengths in cm

y	x	SMA coefficient	<i>Acer grandidentatum</i>	<i>Amelanchier alnifolia</i>	<i>Betula occidentalis</i>	<i>Cornus sericea</i>	<i>Populus fremontii</i>	<i>Symphoricarpos oreophilus</i>	Common exponent (CI)	Pairwise differences
\bar{A}	A_{twig}	Multiplier	1.69	0.92	1.26	0.88	1.18	0.26	0.61 (0.59–0.64)	0
		Exponent	0.59	0.64	0.61	0.60	0.56	0.66		
\bar{A}	n	Multiplier	5.43	1.58	3.71	1.68	2.26	0.066	1.16 (1.07–1.25)*	1
		Exponent	1.13	1.33	0.93	1.09	1.08	1.43		
A_{twig}	n	Multiplier	7.21	2.32	5.90	2.93	3.15	0.12	1.90 (1.81–1.99)**	2
		Exponent	1.91	2.06	1.52	1.81	1.90	2.17		
\bar{A}	l_{twig}	Multiplier	15.3	8.08	8.58	4.27	7.86	0.73	0.50 (0.47–0.54)***	4
		Exponent	0.51	0.41	0.35	0.54	0.61	0.54		
\bar{A}	d_{twig}	Multiplier	4.37	4.16	2.46	4.49	2.87	1.52	1.73 (1.63–1.84)***	6
		Exponent	2.09	1.67	2.41	1.60	1.67	1.24		
n	l_{twig}	Multiplier	2.51	3.43	2.48	2.35	3.19	5.40	0.42 (0.39–0.44)***	5
		Exponent	0.45	0.31	0.38	0.49	0.57	0.38		
A_{twig}	l_{twig}	Multiplier	41.6	29.6	23.5	13.8	28.6	4.76	0.82 (0.78–0.87)***	9
		Exponent	0.87	0.63	0.58	0.89	1.08	0.82		
A_{twig}	d_{twig}	Multiplier	4.99	10.5	3.01	14.9	4.80	14.4	2.89 (2.74–3.06)***	8
		Exponent	3.54	2.61	3.97	2.66	2.96	1.89		
n	d_{twig}	Multiplier	0.82	2.08	0.64	2.45	1.25	8.99	1.49 (1.39–1.60)***	9
		Exponent	1.86	1.26	2.61	1.46	1.56	0.87		
l_{twig}	d_{twig}	Multiplier	0.087	0.19	0.029	1.09	0.19	3.84	3.32 (3.10–3.56)***	10
		Exponent	4.09	4.13	6.84	2.97	2.73	2.29		

Common exponent significance: * $P < 0.05$; ** $P < 0.01$; *** $P < 0.001$.

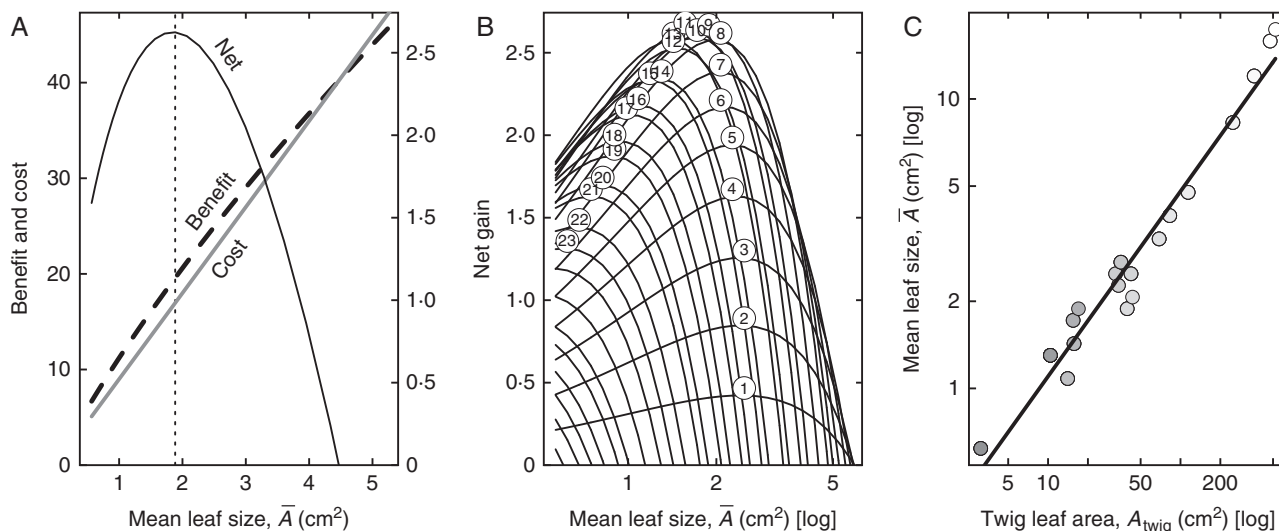


FIG. 4. Example of optimal \bar{A} , n and A_{twig} selection and \bar{A} versus A_{twig} scaling. (A) With constant twig leaf number ($n = 9$) and increasing mean leaf size, the total benefit (dashed line) increases faster and then slower than total cost (grey line), leading to an optimal \bar{A} (vertical line) which maximizes net gain (solid black line). Shown are model data for twigs under a canopy with $\text{LAI}_{\text{can}} = 3.8$, $f_{\text{eff}} = 0.24$, $c_0 = 3.1$ and $\beta = 1$. (B) For increasing n (numbers at peaks) each n has an optimal \bar{A} and across n there is an optimal $\bar{A} : n$ pair (1.7:9 here). Model conditions as above. (C) The optimal \bar{A} and n (and hence A_{twig}) increases with increasing canopy openness (lighter symbol shades denote greater openness). Model conditions are as above, but twig self-shading varied curvilinearly from $f_{\text{eff,open}} = 0.05$ to $f_{\text{eff,closed}} = 0.5$, which produced $b_1 = 0.64$.

markedly so when self-shading decreased linearly with canopy openness (Fig. 5D).

When using decussate phyllotaxy, within-twig variation in leaf size, or circular leaves, the model produced patterns of \bar{A} by A_{twig} scaling exponents similar to those in Fig. 5 (not shown). Mean exponents from these variants plotted against exponents from the standard model did not deviate significantly from the 1:1 line ($P > 0.1$, $P > 0.2$ and $P > 0.7$, respectively) when testing for common SMA slopes and elevations.

Making cost/area a function of light absorption had negligible effect on \bar{A} versus A_{twig} exponents. When leaves absorbing the maximum amount of light cost twice as much [$a_3 = 1$ in eqn (7)], mean exponents increased or decreased (maximum change = +0.003) in the scenario represented by closed circles in Fig. 5D. Increasing to $a_3 = 3$ (up to 4-fold greater cost) had essentially no additional effect. Greater maximum cost did, however, result in a higher selected c_0 range to compensate.

DISCUSSION

We recast Corner's rule (1949) as the prediction that larger leaves correlate positively with greater twig leaf area. Not only was this prediction supported within measured species, but the \bar{A} versus A_{twig} scaling exponents (b_1) were more similar across species than the scaling of other twig properties. In the six study species, all b_1 values were significantly less than 1 and they clustered around 0.6, indicating specific coordination between \bar{A} and leaf number. Furthermore, our model supported Corner's rule and provided an answer to the question: why do thick twigs not support small leaves? The answer is: given that thicker twigs are necessary to support the hydraulic and mechanical demands of greater A_{twig} , partitioning that larger A_{twig} into few, large leaves produces a better return on investment than many

small leaves. Consistent with this observation, Duursma *et al.* (2012) showed that, for a given whole plant leaf area, larger leaves are spatially more dispersed (i.e. fewer leaves per twig) and attain greater light interception efficiency.

The model predicted that exponent b_1 is a function of twig self-shading and leaf cost/area relationships. When twig self-shading was constant across all modelled canopy structures, the model generally predicted b_1 at or near isometry (i.e. constant n ; Fig. 5B). The tendency for constant n can be explained by the geometry of spiral phyllotaxy. When divergence between leaves is the exact golden angle, leaves will never perfectly overlap. But once the leaves have covered one rotation, additional leaves fill increasingly small gaps left by the leaves above. When the potential benefit increases (via greater c_0 or a less dense canopy with larger openings) it is generally more beneficial to fill the opening by increasing \bar{A} than it is to increase n . This results in nearly constant n and, therefore, $b_1 \approx 1$. This is consistent with models showing little benefit of the golden angle over other phyllotactic angles (Valladares and Brites, 2004). Reducing twig self-shading under all canopies allowed more light to reach these lower leaves and favour greater n , but the effect was the same across environments, which maintained b_1 near isometry.

There was a tendency for the model to predict b_1 somewhat greater than 1 when twig self-shading was the same under all canopies (Fig. 5B). This corresponds to fewer, larger leaves in more open canopies. The reason for this is related to the rate of decline in available light away from the twig centre [i.e. $\bar{\tau}_{\text{can,pxl}}$ in eqn (3); Fig. 1E, F]. Suppose the most open canopy favours a particular $\bar{A} : n$ pair. This canopy has a gradual decline in $\bar{\tau}_{\text{can,pxl}}$ moving away from the centre of its large openings (Fig. 1E), so large \bar{A} is favoured over large n . For the dense canopy with smaller openings, however, $\bar{\tau}_{\text{can,pxl}}$ drops quickly to its minimum (Fig. 1F). This curve is likely steep enough to make

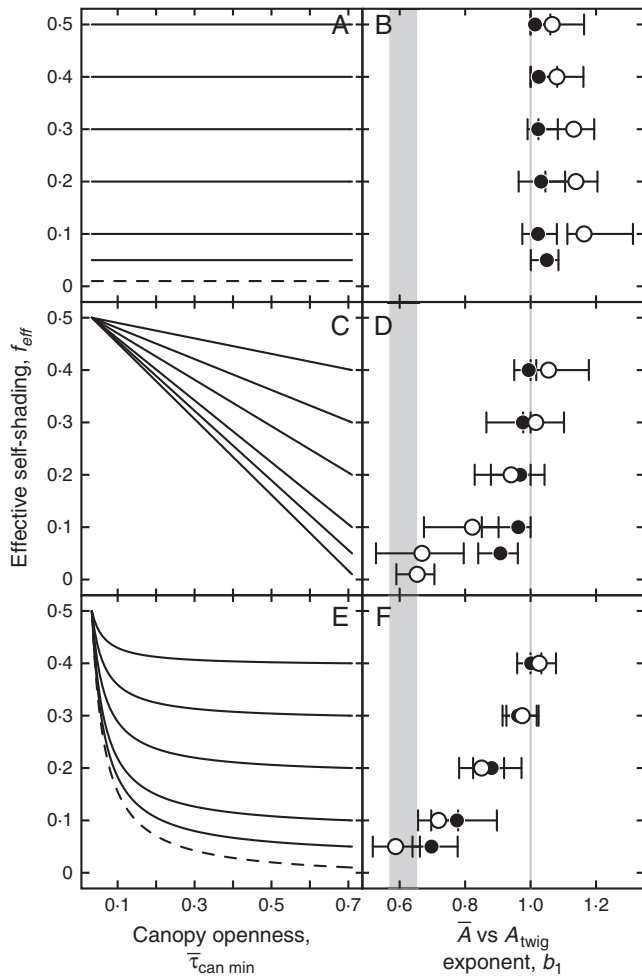


Fig. 5. Self-shading versus canopy openness scenarios (left panels) next to corresponding \bar{A} versus A_{twig} scaling exponents (right panels). We considered scenarios where, as canopy openness increased, twig self-shading was constant (A, B), decreased linearly (C, D) or decreased curvilinearly (E, F). Symbols represent the mean and bars the range. Exponents are shown relative to isometry (grey line) and the observed range (grey bar). Leaf cost per area was either constant ($\beta=1$; black circles) or increased with size ($\beta=1.1$; open circles). Dashed lines in left-hand panels indicate modelled scenarios that did not meet scaling criteria. Selectively reducing self-shading in more open canopies was necessary to predict the observed exponents.

increasing n more beneficial than increasing \bar{A} , resulting in more leaves in the closed versus open canopy and $b_1 > 1$. When larger leaves cost more per area (i.e. $\beta > 1$), b_1 became even steeper (Fig. 5B). Increasing β from 1 to 1.1 favoured more leaves under all canopies but more so under denser canopies. It is likely that the constraint on leaf size in low light leads these twigs to favour an even larger number of small leaves when they are cheaper.

Altering self-shading across canopy structures was necessary to favour $b_1 < 1$, as observed in the study species. Selectively reducing twig self-shading under more open canopies allowed these high-light environments that already favour larger \bar{A} to also favour greater n . Keeping self-shading high in closed canopies maintained smaller n with smaller \bar{A} . The exponent b_1 was further reduced when $\beta > 1$ (Fig. 5D, F). Making larger leaves

more expensive favours smaller \bar{A} and greater n . This was especially true under more open canopies with low self-shading and large leaves. According to the model, our observed common exponent of $b_1 = 0.61$ should be associated with less self-shading in larger versus smaller twigs across all the study species, perhaps in combination with a greater specific cost of larger leaves. Although beyond the scope of the present study, this very specific hypothesis is testable with measurements of twig and canopy light distribution and specific leaf areas.

The traditional assessment of Corner rule (\bar{A} versus d_{twig}) produced much more varied exponents than \bar{A} by A_{twig} scaling. Interestingly, \bar{A} by d_{twig} exponents covaried with A_{twig} by d_{twig} exponents. The \bar{A} by A_{twig} exponent can be represented by how \bar{A} and A_{twig} scale with d_{twig} . For example, in *Acer* we observed $\bar{A} \propto d_{\text{twig}}^{2.09}$ and $A_{\text{twig}} \propto d_{\text{twig}}^{3.54}$, making $\bar{A} \propto A_{\text{twig}}^{0.59} = 2.09/3.54$. This mathematical relationship makes it apparent that, although \bar{A} by d_{twig} and A_{twig} by d_{twig} scaling exponents seemed to vary widely (1.24–2.41 and 1.89–3.97, respectively), their ratios remained around 0.6. This apparent coordination to produce $b_1 \approx 0.6$ supports our hypothesis that \bar{A} versus A_{twig} scaling is more fundamental to Corner's rule than the scaling of either \bar{A} or A_{twig} with twig size.

Our data only represent species from one functional type and one environment. Additional studies will reveal whether other functional groups in other environments share an \bar{A} versus A_{twig} exponent and whether it equals 0.6 or varies systematically and with light environment as predicted by our model. We were unable to find any other study that reported \bar{A} by A_{twig} scaling intraspecifically. It seems that this more fundamental basis for Corner's rule has been largely overlooked. We did find a single intraspecific study, however, where we could deduce \bar{A} by A_{twig} scaling from the reported SMA scaling of both areas with d_{twig}^2 . Preston and Ackerly (2003) reported individual A_{twig} by d_{twig}^2 exponents and a common \bar{A} by d_{twig}^2 exponent for 12 California species from three genera and contrasting environments. From these data, we calculated intraspecific b_1 between 0.64 and 0.90 (mean = 0.76), with steeper slopes slightly favoured by xeric (versus mesic) species. These exponents are consistent with model predictions when self-shading declines moderately to steeply with greater canopy openness (Fig. 5C–F), but it is difficult to infer how the canopy light environment varied across these species.

There are several interspecific studies where \bar{A} by A_{twig} scaling could be deduced by the same approach or from reported \bar{A} and A_{twig} species means. These data are difficult to interpret because, as our study demonstrated, the a_1 multiplier can vary across species, causing inter- and intraspecific exponents to differ. Similar inter- versus intraspecific discrepancies in leaf scaling were found by Dombroskie and Aarssen (2012). Nevertheless, many of these interspecific inferences are broadly consistent with the trends suggested by our model. Data from White (1983a) indicate that b_1 was steeper among shade-tolerant species ($b_1 = 1.33$), where denser canopies could reduce variation in self-shading, than among intermediate (1.05) and intolerant (0.85) species, where self-shading could be more variable. White's (1983b) other study was consistent with a markedly steeper scaling in evergreen angiosperms ($b_1 = 1.14$), whose broader leaves may cause more consistent self-shading than the needle leaves of evergreen gymnosperms ($b_1 = 0.68$). Falster and Westoby's (2003) data also indicate steeper scaling

under higher leaf cover ($b_1 = 1.53$) versus low (1.37), but the difference was not significant. Other interspecific studies were less obviously relatable to light environments (Westoby and Wright, 2003; Yang *et al.*, 2009; Liu *et al.*, 2010). Interspecific SMA exponents are likely to be steeper than intraspecific ones because of lower r values that result from differing a_1 multipliers. As in our study, the interspecific data tended to show more variation in \bar{A} by d_{twig} and A_{twig} by d_{twig} exponents than in b_1 .

The model results were encouraging and suggestive that optimizing the investment in leaves, as we have defined it, is an important control on leaf size and number. However, the model could be extended to broaden its applicability. The model consistently predicts larger leaves in larger canopy openings, a trend that ignores potential energy-balance problems of large leaves in too much light (Givnish, 1987; Long *et al.*, 1994; Pearcy *et al.*, 2005). The model also does not account for changes in leaf angle that alter light interception independently of leaf size (Pearcy *et al.*, 2005). Furthermore, the assumption that twigs always target canopy openings biases the analysis towards twigs growing into the canopy periphery, or growing in relatively open canopies (typical ‘sun’ leaves). Hence the model fails to predict the general observation of larger ‘shade’ leaves found in the more uniform shade beneath dense canopies (Sack *et al.*, 2003, 2006; Nardini *et al.*, 2012) and across species (Niinemets and Kull, 1994; Bragg and Westoby, 2002). Running the model for uniform light (i.e. no spatial autocorrelation of light associated with canopy openings) does increase optimal leaf size (not shown), and adding energy-balance penalties would extend the model to the qualitative differences in light environments of classic sun versus shade leaves (Hanson, 1917; Sack *et al.*, 2006). Energy balance may help explain differences in \bar{A} versus A_{twig} scaling multipliers across species. Compared with the other five species, *Symphoricarpos* had a notably lower \bar{A} versus A_{twig} multiplier (more leaves at a given A_{twig} ; Fig. 2). At a given d_{twig} this species had longer twigs (Table 1) and less sapwood (Smith and Sperry, 2014), yet similar A_{twig} (Fig. 3B). These factors suggest poorer hydraulic supply to each leaf and therefore reduced capacity for evaporative cooling. In this context, partitioning A_{twig} into smaller leaves may be necessary to reduce heat load. Additionally, the model as applied here does not predict changes in leaf size across environments with contrasting water supply or soil fertility (Givnish, 1987; Cunningham *et al.*, 1999). These shortcomings could specifically be addressed by extending the model to more explicitly define multipliers c_0 and c_1 in terms of structural and physiological characteristics of leaves.

We have identified a fundamental corollary of Corner’s rule that is supported empirically and theoretically. The specific predictions of the economics model are eminently testable, because the driving variables of canopy openness and twig self-shading (Figs 1 and 5) can be measured with arrays of light sensors within twigs and canopies. The simplicity of the question and the minimal data requirements should inspire further evaluation of why thick twigs should support large leaves.

SUPPLEMENTARY DATA

Supplementary data are available online at www.aob.oxfordjournals.org and consist of the following: dataset of the accessions used in the study.

ACKNOWLEDGEMENTS

We thank Jon Seger for input that led to the economics model concept; David Ackerly, Remko Duursma and two other reviewers for useful comments on earlier versions of this manuscript; and David Love for assistance with data collection in 2011. This work was supported by NSF (IBN-0743148).

LITERATURE CITED

- Bragg JG, Westoby M. 2002. Leaf size and foraging for light in a sclerophyll woodland. *Functional Ecology* **16**: 633–639.
- Brouat C, Gibernau M, Amsellem L, McKey D. 1998. Corner’s rules revisited: ontogenetic and interspecific patterns in leaf-stem allometry. *New Phytologist* **139**: 459–470.
- Campbell GS, Norman JN. 1998. *An introduction to environmental biophysics*, 2nd edn. New York: Springer.
- Corner EJH. 1949. The durian theory of the origin of the modern tree. *Annals of Botany* **13**: 368–414.
- Cunningham SA, Summerhayes B, Westoby M. 1999. Evolutionary divergences in leaf structure and chemistry, comparing rainfall and soil nutrient gradients. *Ecological Monographs* **69**: 569–588.
- Dombroskie SL, Aarssen LW. 2012. The leaf size/number trade-off within species and within plants for woody angiosperms. *Plant Ecology and Evolution* **145**: 38–45.
- Duursma RA, Falster DS, Valladares F, *et al.*, 2012. Light interception efficiency explained by two simple variables: a test using a diversity of small-to medium-sized woody plants. *New Phytologist* **193**: 397–408.
- Eloy C. 2011. Leonardo’s rule, self-similarity, and wind-induced stresses in trees. *Physical Review Letters* **107**: 1–5.
- Evans JR, Poorter H. 2001. Photosynthetic acclimation of plants to growth irradiance: the relative importance of specific leaf area and nitrogen partitioning in maximizing carbon gain. *Plant, Cell & Environment* **24**: 755–767.
- Falster DS, Westoby M. 2003. Leaf size and angle vary widely across species: what consequences for light interception? *New Phytologist* **158**: 509–525.
- Farnsworth KD, Van Gardingen PR. 1995. Allometric analysis of Sitka spruce branches: mechanical versus hydraulic design principles. *Trees - Structure and Function* **10**: 1–12.
- Givnish TJ. 1987. Comparative studies of leaf form: assessing the relative roles of selective pressures and phylogenetic constraints. *New Phytologist* **106**: 131–160.
- Hanson HC. 1917. Leaf-structure as related to environment. *American Journal of Botany* **4**: 533–560.
- Heusner AA. 1982. Energy and metabolism I. Is the 0.75 mass exponent of Kleiber’s equation a statistical artifact? *Respiration Physiology* **48**: 1–12.
- Honda H, Fisher JB. 1978. Tree branch angle: maximizing effective leaf area. *Science* **199**: 888–889.
- Judd WS, Campbell CS, Kellogg EA, Stevens PF, Donoghue MJ. 2008. *Plant systematics: a phylogenetic approach*, 3rd edn. Sunderland, MA: Sinauer Associates.
- Liu Z, Cai Y, Li K, Guo J. 2010. The leaf size-twig size spectrum in evergreen broadleaved forest of subtropical China. *African Journal of Biotechnology* **9**: 3382–3387.
- Long SP, Humphries S, Falkowski PG. 1994. Photoinhibition of photosynthesis in nature. *Annual Review of Plant Physiology and Plant Molecular Biology* **45**: 633–662.
- McMahon TA, Kronauer RE. 1976. Tree structures: deducing the principle of mechanical design. *Journal of Theoretical Biology* **59**: 443–466.
- Milla R, Reich PB. 2007. The scaling of leaf area and mass: the cost of light interception increases with leaf size. *Proceedings of the Royal Society B: Biological Sciences* **274**: 2109–2114.
- Nardini A, Pedá G, Salleo S. 2012. Alternative methods for scaling leaf hydraulic conductance offer new insights into the structure-function relationships of sun and shade leaves. *Functional Plant Biology* **39**: 394–401.
- Niinemets Ü, Kull K. 1994. Leaf weight per area and leaf size of 85 Estonian woody species in relation to shade tolerance and light availability. *Forest Ecology and Management* **70**: 1–10.
- Niinemets Ü, Portsmuth A, Tena D, Tobias M, Matesanz S, Valladares F. 2007. Do we underestimate the importance of leaf size in plant economics? Disproportional scaling of support costs within the spectrum of leaf physiognomy. *Annals of Botany* **100**: 283–303.

- Niinemets Ü, Keenan TF, Hallik L. 2015. A worldwide analysis of within-canopy variations in leaf structural, chemical and physiological traits across plant functional types. *New Phytologist* **205**: 973–993.
- Olson ME, Aguirre-Hernández R, Rosell JA. 2009. Universal foliage-stem scaling across environments and species in dicot trees: plasticity, biomechanics and Corner's rules. *Ecology Letters* **12**: 210–219.
- Pearcy RW, Muraoka H, Valladares F. 2005. Crown architecture in sun and shade environments: assessing function and trade-offs with a three-dimensional simulation model. *New Phytologist* **166**: 791–800.
- Posada JM, Lechowicz MJ, Kitajima K. 2009. Optimal photosynthetic use of light by tropical tree crowns achieved by adjustment of individual leaf angles and nitrogen content. *Annals of Botany* **103**: 795–805.
- Preston KA, Ackerly DD. 2003. Hydraulic architecture and the evolution of shoot allometry in contrasting climates. *American Journal of Botany* **90**: 1502–1512.
- R Core Team. 2014. *R: a language and environment for statistical computing*. Vienna, Austria: R Foundation for Statistical Computing. <http://www.R-project.org/>.
- Sack L, Cowan PD, Jaikumar N, Holbrook NM. 2003. The 'hydrology' of leaves: coordination of structure and function in temperate woody species. *Plant, Cell & Environment* **26**: 1343–1356.
- Sack L, Melcher PJ, Liu WH, Middleton E, Pardee T. 2006. How strong is intracanalopy leaf plasticity in temperate deciduous trees? *American Journal of Botany* **93**: 829–839.
- Smith DD, Sperry JS. 2014. Coordination between water transport capacity, biomass growth, metabolic scaling and species stature in co-occurring shrub and tree species. *Plant, Cell & Environment* **37**: 2679–2690.
- Sone K, Suzuki AA, Miyazawa S, Noguchi K, Terashima I. 2009. Maintenance mechanisms of the pipe model relationship and Leonardo da Vinci's rule in the branching architecture of *Acer rufinerve* trees. *Journal of Plant Research* **122**: 41–52.
- Valladares F, Brites D. 2004. Leaf phyllotaxis: does it really affect light capture? *Plant Ecology* **174**: 11–17.
- Villar R, Merino J. 2001. Comparison of leaf construction costs in woody species with differing leaf life-spans in contrasting ecosystems. *New Phytologist* **151**: 213–226.
- Warton DI, Duursma RA, Falster DS, Taskinen S. 2012. smatr 3 – an R package for estimation and inference about allometric lines. *Methods in Ecology and Evolution* **3**: 257–259.
- Westoby M, Wright IJ. 2003. The leaf size-twig size spectrum and its relationship to other important spectra of variation among species. *Oecologia* **135**: 621–628.
- White PS. 1983a. Corner's rules in eastern deciduous trees: allometry and its implications for the adaptive architecture of trees. *Bulletin of the Torrey Botanical Club* **110**: 203–212.
- White PS. 1983b. Evidence that temperate east North American evergreen woody plants follow Corner's rules. *New Phytologist* **95**: 139–145.
- Wright IJ, Falster DS, Pickup M, Westoby M. 2006. Cross-species patterns in the coordination between leaf and stem traits, and their implications for plant hydraulics. *Physiologia Plantarum* **127**: 445–456.
- Yang D, Li G, Sun S. 2009. The effects of leaf size, leaf habit, and leaf form on leaf/stem relationships in plant twigs of temperate woody species. *Journal of Vegetation Science* **20**: 359–366.
- Yang X, Yan E, Chang SX, Wang X, Zhao Y, Shi Q. 2014. Twig-leaf size relationships in woody plants vary intraspecifically along a soil moisture gradient. *Acta Oecologica* **60**: 17–25.